Contrib Mineral Petrol (2002) 142: 666–678
DOI 10.1007/s00410-001-0328-3

Don R. Baker · Aida Maria Conte
Carmela Freda · Luisa Ottolini

The effect of halogens on Zr diffusion and zircon dissolution in hydrous metaluminous granitic melts

Received: 20 December 2000 / Accepted: 25 September 2001 / Published online: 6 December 2001

Abstract Diffusion of Zr and zircon solubility in hydrous, containing approximately 4.5 wt% H_2O, metaluminous granitic melts with halogens, either 0.35 wt% Cl (LCl) or 1.2 wt% F (MRF), and in a halogen-free melt (LCO) were measured at 1.0 GPa and temperatures between 1,050 and 1,400 °C in a piston-cylinder apparatus using the zircon dissolution technique. Arrhenius equations for Zr diffusion in each hydrous melt composition are, for LCO with 4.4 ± 0.4 wt% H_2O: $D = 2.88 \pm 0.03x10^{-8} \exp\left(\frac{-140.1 \pm 33.9}{RT}\right)$, for LCl with 4.5 ± 0.5 wt% H_2O: $D = 2.33 \pm 0.05x10^{-4} \exp\left(\frac{-254.8 \pm 64.1}{RT}\right)$ and for MRF with 4.9 ± 0.3 wt% H_2O: $D = 2.54 \pm 0.03x10^{-5} \exp\left(\frac{-223.8 \pm 15.5}{RT}\right)$.

Solubilities determined by the dissolution technique were reversed for LCO $+4.5 \pm 0.5$ wt% H_2O by crystallization of a Zr-enriched glass of LCO composition at 1,200 and 1,050 °C at 1.0 GPa. The solubility data were used to calculate partition coefficients of Zr between zircon and hydrous melt, which are given by the following expressions: for LCO $\ln D_{Zr}^{zircon/melt} = 1.63\left(\frac{10000}{T}\right) - 5.87$, for LCl $\ln D_{Zr}^{zircon/melt} = 1.47\left(\frac{10000}{T}\right) - 4.75$ and, for MRF by $\ln D_{Zr}^{zircon/melt} = 1.47\left(\frac{10000}{T}\right) - 4.91$.

Experiments on the same compositions, but with water contents down to 0.5 wt%, demonstrated reductions in both the diffusion coefficient of Zr and zircon solubility in the melt. The addition of halogens at the concentration levels studied to metaluminous melts has a small effect on either the diffusion of Zr in the melt, or the solubility of zircon at all water concentrations and temperatures investigated. At 800 °C, the calculated diffusion coefficient of Zr is lowest in LCl, 9×10^{-17} m^2 s^{-1}, and is highest in LCO, 4×10^{-15} m^2 s^{-1}. Extrapolation of the halogen-free solubility data to a magmatic temperature of 800 °C yields solubilities of approximately one-third of those directly measured in similar compositions, predicted by earlier studies of zircon dissolution and based upon analyses of natural rocks. This discrepancy is attributed to the higher oxygen fugacity of the experiments of this study compared with previous studies and nature, and the effect of oxygen fugacity on the structural role of iron in the melt, which, in turn, affects zircon solubility, but does not significantly affect Zr diffusion.

D.R. Baker (✉) · C. Freda
Earth and Planetary Sciences,
McGill University, 3450 rue University,
Montréal, QC H3A 2A7, Canada
E-mail: donb@eps.mcgill.ca

A.M. Conte
CNR-CS per gli Equilibri
Sperimentali in Minerali e Rocce,
c/o Dipartimento di Scienze della Terra,
Università degli Studi ''La Sapienza'',
P.le Aldo Moro, 5, I-00185 Roma, Italy

L. Ottolini
CNR-CS per la Cristallochimica e la Cristallografia,
Via Ferrata, 1, I-27100 Pavia, Italy

Extra address: C. Freda
Istituto Nazionale di Geofisica
e Vulcanologia, Via di Vigna Murata,
605, 00143 Roma, Italy

Editorial responsibility: T.L. Grove

Introduction

Granitic and rhyolitic magma systems generally contain a rich assemblage of accessory minerals such as zircon, apatite, titanite, monazite and allanite that control the abundance of rare earth elements (REE) and high field strength elements (HFSE). Numerous studies, both classic (e.g. Hanson 1978; Fourcade and Allegre 1981; Miller and Mittlefehldt 1982; Mittlefehldt and Miller 1983) and recent (e.g. Hoskin et al. 2000), have shown that minute quantities of such accessory minerals often contain most of the HFSE in felsic rocks. Previous studies on the dissolution of zircon, apatite and monazite and on the diffusion of their essential struc-

tural components in felsic melts constrain the effect of these minerals on the trace element chemistry of hydrous granitic melts (Watson 1979, 1980; Watson and Capobianco 1981; Watson and Green 1981; Green and Watson 1982; Harrison and Watson 1983, 1984; Watson and Harrison 1983; Rapp and Watson 1986; Keppler 1993).

Among accessories, zircon has been of major interest to geochemists because it is a major sink of Zr, Hf, Th, Ta and REE in granites and because of its role in U–Pb geochronology (e.g. Pidgeon et al. 1996, 1998; Nasdala et al. 1998; Eichorn et al. 2000). Several experimental studies have investigated zircon solubility and dissolution rate in natural and synthetic silicate melts (Larsen 1973; Watson 1979; Watson and Harrison 1983; Keppler 1993). These studies provide information on zircon crystallization in magmatic systems and on its tendency to survive or to be consumed during crustal melting events. The extremely low solubility of zircon in hydrous metaluminous and peraluminous granitic melts (~100 ppm at 750 °C) lead Watson and Harrison (1983) to conclude that solid state diffusion is responsible for the reallocation of trace elements between zircon and melt, and that Zr diffusion in felsic melts is the rate-limiting step for the dissolution of zircons. In their companion study, Harrison and Watson (1983) investigated the role of variable water content on the kinetics of zircon dissolution in felsic systems. Remarkable contrasts arise between wet and dry behaviour. The first 2 wt% H_2O introduced in the felsic melt is critical because it increases the zirconium diffusivity at 1,200 °C by a factor of 100 and doubles its solubility; this indicates that with respect to dry conditions dissolution proceeds geologically instantaneously in water-bearing, but undersaturated, felsic melts.

A critical factor in trace element models for HFSE and REE in granite petrogenesis may be the role played by halogens. The influence of halogens on HFSE and REE concentrations during granite petrogenesis has been suggested because of the observed correlation between HFSE and halogen contents (Pichavant et al. 1987; Pollard et al. 1987; Congdon and Nash 1991; Štemprok 1991). Although transport of HFSE via formation of fluorine complexes in an aqueous fluid phase has been hypothesized, this process has not been supported by experimental evidence for many HFSE (London 1987; Keppler and Wyllie 1990, 1991). It has been suggested, however, that the formation of fluorine complexes in the melt could drastically change the fractionation behaviour of HFSE between melt and crystals, thus resulting in a correlation between fluorine and HFSE (Raimbault et al. 1987). Although analyses of granitic rocks for both halogens and zirconium are rare, examination of 120 analyses of granites and rhyolites demonstrates that the rocks most enriched in Zr are also substantially enriched in either F or Cl (Hildreth 1981; Mutschler et al. 1981; Conrad 1984; Hildreth et al. 1984, 1991; Rytuba and McKee 1984; Hervig and Dunbar 1992). Notably, many Zr-enriched silicic rocks, those with more than approximately 200 ppm Zr, are peralkaline.

The effect of F on zircon solubility in felsic melts was investigated by Keppler (1993) who found a strongly non-linear solubility in a water-saturated haplogranitic melt containing 0–6 wt% F, qualitatively consistent with the trends seen in natural rocks. In agreement with Watson (1979) and Watson and Harrison (1983), Keppler demonstrated that the solubility of zircon is extremely low in hydrous, metaluminous silicic melts and in melts with 2 wt%, or less, F at 800 °C, 200 MPa.

This paper reports an experimental investigation of zircon solubility and Zr diffusion in metaluminous felsic melts containing between 0.4 and 5.1 wt% H_2O and amounts of F (1.2 wt%) and Cl (0.35 wt%) typical of F- and Cl-enriched natural metaluminous felsic rocks (Pichavant et al. 1987; Congdon and Nash 1991; Štemprok 1991). This study complements earlier ones by Harrison and Watson (1983) and Keppler (1993) on zircon saturation.

Experimental techniques

Zircon solubility and Zr diffusion were determined using the zircon dissolution technique pioneered by Harrison and Watson (1983). Diffusion/dissolution experiments contained zircon, one of three felsic glass compositions (Table 1) and water. The first glass was the same metaluminous rhyolitic obsidian (LCO) used by Harrison and Watson (1983). The second was a chlorine-containing mix (LCl, 0.35 wt% Cl) obtained by combining LCO with $PtCl_4$ (1.26 wt%), and the third was rhyolitic glass (MRF) containing 1.2 wt% fluorine synthesized by Baker and Vaillancourt (1995). Based upon experiments performed in this laboratory and by Webster (1992), the chlorine concentration in LCl is close to the value at which a metaluminous melt with 6 wt% H_2O saturates in a second phase (either molten hydrous chloride or a Cl-bearing hydrous fluid). This chlorine concentration far exceeds that measured in most granitic and rhyolitic rocks. Because of the high partition coefficient of Cl between fluid and melt (Carroll and Webster 1994) we cannot be certain of the pre-eruptive Cl concentrations, but we can presume they did not exceed the Cl solubility in the melt. The fluorine concentration in MRF is far below the maximum solubility of F in a metaluminous granitic melt (Carroll and Webster 1994); however, it is significantly above the F concentration analysed in most granitic and rhyolitic rocks (Carroll and Webster 1994).

Two additional melt compositions were synthesized by doping LCO with ZrO_2 (LCOZr) or ZrO_2 + Fe_2O_3 (LCOZrFe). These compositions were synthesized in order to perform reversals of the dissolution experiments by the crystallization of zircon. Each mix was ground under ethanol for 30 min then melted twice, with intermediate grinding, at 1,500 °C for 4 h each time. Both starting materials contained glass with a small amount, less than ~10% by volume, of crystals whose maximum

Table 1 Starting glass compositions. Major element contents of starting glasses were analysed by electron microprobe analysis at McGill University. FeO* is total iron analysed as FeO

Oxide	LCO	MRF	LCl
SiO_2	76.37	76.17	75.72
TiO_2	0.11	0.05	0.00
Al_2O_3	13.35	12.48	13.27
FeO*	0.79	1.94	1.06
MnO	0.06	0.01	0.00
MgO	0.07	0.04	0.07
CaO	0.51	0.33	0.55
Na_2O	4.31	4.10	4.03
K_2O	4.67	4.54	4.74
F	0.00	1.22[a]	0.11[b]
Cl			0.35[b]
Total	100.24	100.88	99.90
M[c]	1.37	1.35	1.34
FM[d]	1.50	1.69	1.53

[a]O = F is 0.51 wt%
[b]O = F, Cl is 0.046 and 0.079 wt%, respectively
[c]M value calculated from Watson and Harrison (1983)
[d]FM value calculated from Ryerson and Watson (1987)

size was below 6 μm in the longest dimension. Microprobe analysis demonstrated that the glassy portions of these mixes were homogeneous and the crystals were a mixture of residual zirconia and zircon. The Zr concentration in the glassy portion of LCOZr was 19,000 ± 660 ppm. The glassy portion of LCOZrFe contained 4.55 ± 0.10 wt% FeO* (total iron analysed as FeO) and 18,000 ± 490 ppm Zr. No alkali loss occurred in these compositions during their synthesis. These two starting materials glasses were ground under ethanol to a grain size below 50 μm and stored in a drying oven at 110 °C.

Zircon crystals from the Mud Tank Carbonatite, Harte Range, Australia (cf. Harrison and Watson 1983), obtained from Wards Scientific, were cut in 1–3-mm slabs and used in early experiments. Additional crystals of zircon from Colonia, Sri Lanka, purchased from Hawthorneden Minerals, were prepared in the same way. Some of these slabs had crystal faces parallel to the c-axis and were used without additional polishing in the exeriments. For slabs that did not have crystal faces, one side parallel to the c-axis was polished to a 1-μm finish.

Experiments were performed in a piston-cylinder apparatus at 1.0 GPa and temperatures between 1,050 and 1,400 °C. Experiments at temperatures up to 1,200 °C used $Au_{75}Pd_{25}$ capsules whereas those at higher temperatures used Pt capsules. Capsules were loaded with distilled water, approximately either 2 or 5.5 wt%, the starting glass (about 20 mg) and a millimetre-sized slab of zircon oriented with the crystal (or polished) face perpendicular to the capsule walls. Capsules were welded closed in a water bath to avoid volatile loss and placed in an oven at 110 °C for at least 2 h. Capsules were placed into 1.91 cm NaCl-Pyrex glass-crushable alumina assemblies (Hudon et al. 1994) and run for 1 to 43 h. Experimental capsules AA1–AA28 were surrounded only by alumina powder. Water analyses of quenched melts in these capsules demonstrated severe water loss in many cases. Therefore, sample capsules AA29 and higher were surrounded by a thin layer, ~10 mg, of pyrophyllite powder in the assembly to reduce water loss (Freda et al. 2001). Experiments were heated and pressured simultaneously to an overpressure of 0.2 GPa and then pressure was reduced to 1.0 GPa and held within 0.1 GPa of this value during the experiment. The observed temperatures were controlled within 2 °C of the set point except at the beginning of the experiment when the set point was exceeded by a maximum of 10 °C. Type C thermocouples were used and temperature gradients along the capsules were less than 15 °C (Hudon et al. 1994). Almost all experiments were quenched isobarically to below-solidus temperatures to reduce formation of quench bubbles and crystals; however, even non-isobarically quenched samples did not contain quench bubbles or crystals.

Quenched capsules were mounted longitudinally in epoxy, then prepared for analysis by ion and electron microprobes. Hydrogen concentrations in the run product glasses were analysed by secondary ion mass spectrometry to determine the water content of the melts. Samples were analysed with a Cameca IMS 4f ion microprobe at CNR-Centro di Studio per la Cristallochimica e la Cristallografia (Pavia) following the procedure described in Ottolini et al. (1995) and Freda et al. (2001). Water contents were calculated from measured hydrogen concentrations as is the practice in SIMS work because this technique cannot distinguish between different H-speciations. Nevertheless, Schaller et al. (1992) found no evidence for the presence of significant quantities of HF in fluorine-bearing hydrous haplogranitic glasses, which suggests that hydrogen is only associated with oxygen atoms in the melts and quenched glasses.

Reproducibility of SIMS analysis, measured on the standards, is typically $\leq \pm 5\%$ relative (1 standard deviation) over a 1-day span. Overall accuracy in these total H_2O analyses is $\sim \pm 10\%$ relative, which represents the agreement among H_2O values of our standards used for calibration (see Freda et al. 2001 for details). Ottolini et al. (1995) showed that the use of energy filtering can significantly reduce matrix effects as well as the H-background, which represent the main limitations of applying SIMS to geological samples. Under controlled experimental conditions, very accurate results (better than ± 10% rel.) are strictly dependent on the reliability of the H_2O data of the standards used in the calibration procedure, which, in turn, implies previous precise and accurate work in the standardization of the standard materials themselves. Both SIMS and infrared spectroscopy (e.g. Newman et al. 1986) require standards analysed by other techniques for the determination of water concentration in silicate glasses; however, when properly calibrated with the appropriate standards both techniques provide precise methods of water determination.

Zirconium contents of the glasses adjacent to the zircon as well as major elements, including F and Cl, were measured using a JEOL 8900 electron microprobe equipped with five spectrometers at an accelerating voltage of 15 kV and a current of 50 nA. Counting times on peaks were 50 s for zirconium and 20 s for all other elements. Counting times on backgrounds were one-half those used on peaks. The beam was in most cases focused to a 10-μm diameter, sometimes it was reduced to 5 μm to increase the number of points for short diffusion profiles. A PETH analysing crystal was used to detect zirconium. All data were reduced using the ZAF correction technique. The instrument was calibrated using zircon (Zr), pantelleritic obsidian (Si, Al, Fe, Na, K and Cl), spessartine (Mn), synthetic glass (F) and basaltic glass (Ti, Mg and Ca) standards. Accuracy was evaluated through analysis of a second pantelleritic obsidian with a Zr concentration of 1,885 ppm, previously measured by XRF. Electron microprobe analysis of this glass yielded a Zr concentration of $1{,}848 \pm 90$ ppm. A minimum of three traverses normal to the zircon/glass interface were taken for each sample; spacing between analytical points was either 10 or 5 μm. Analyses closer than 30 μm to the zircon were not used because of secondary Zr fluorescence from the crystal (Harrison and Watson 1983). In some cases, expansion cracks formed during quenching intercepted the traverses making them unusable for diffusion measurements. For almost every sample, multiple traverses were averaged together to calculate Zr diffusion and zircon solubility, but in a few cases only one analytical traverse was successful. Nevertheless, because we performed more than one experiment at a given temperature, a minimum of two traverses at each temperature were used for the determination of Zr diffusion and zircon solubility.

Zirconium concentration profiles produced in experiments (e.g. Fig. 1a) were used to determine Zr diffusion coefficients. Data were computed assuming a geometry in which the glass is considered a semi-infinite reservoir initially at a fixed concentration and the zircon–glass interface (located at distance $x=0$) as a fixed plane at constant composition. The zircon dissolution during the experiment involved a portion of the mineral short enough with respect to the length of the diffusion profile for this assumption to be valid. The Zr diffusion coefficient and its concentration in the melt at zircon saturation, C_o, for this geometry can be calculated from the following solution to Fick's second law:

$$\frac{C_{x,t} - C_o}{C_{bkg} - C_o} = erf\left(\frac{x}{2\sqrt{Dt}}\right)$$

where $C_{x,t}$ is the concentration at distance x from the interface at time t (the experiment run duration), and C_{bkg} is the Zr concentration in the melt at infinite distance away from the crystal (Crank 1975).

The solution to this equation adopted here is similar to that proposed by Harrison and Watson (1983). The model requires that the data be linearized by inversion of the error function (Fig. 1b):

$$\frac{x}{2\sqrt{Dt}} = erf^{-1}\left(\frac{C_{x,t} - C_o}{C_{bkg} - C_o}\right)$$

where C_o is a variable that must be estimated. The inverse error function for each value of $\left(\frac{C_{x,t}-C_o}{C_{bkg}-C_o}\right)$ is plotted against x and the best fit line to the data is determined. The C_o value producing a y intercept close to zero is the best estimate of solubility. The slope of

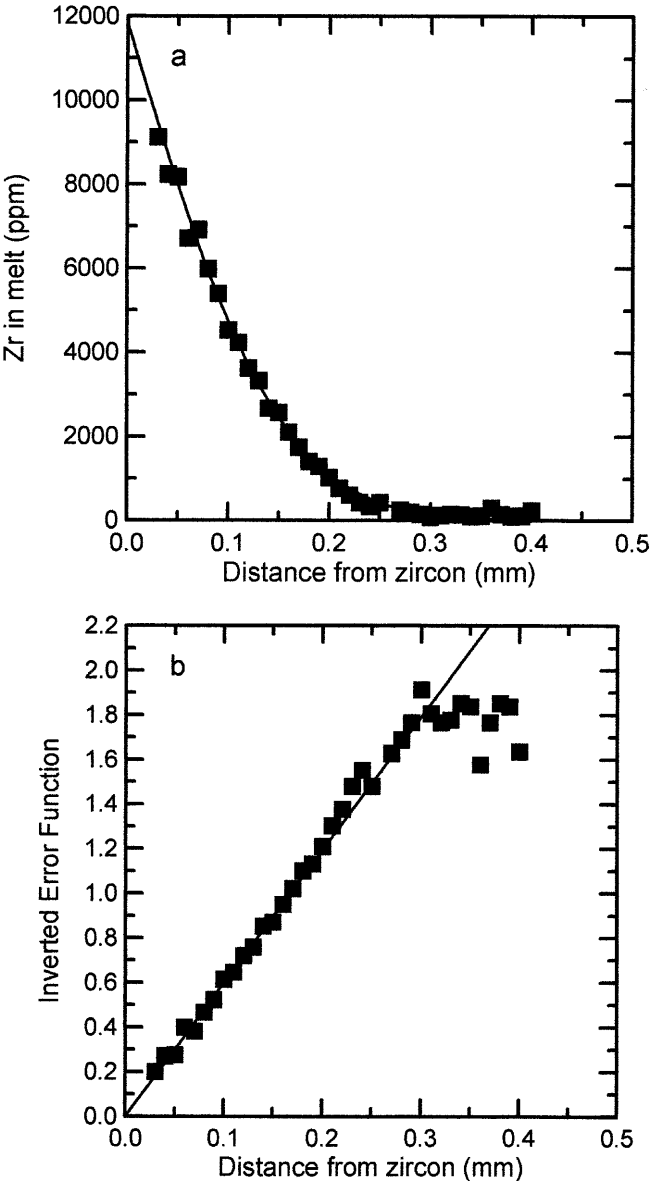

Fig. 1 **a, b** Zirconium diffusion profile (AA50) and error function inversion of the profile. *Solid squares* are **a** measured Zr concentrations and **b** inverted concentrations as a function of distance from the zircon/melt interface. The *solid line* in **a** is theoretical diffusion profile based upon the fit to the error function inversion of **b**, which used only the data points above the background Zr concentration of the melt, and is reached in this experiment at approximately 0.2 mm away from the zircon. See text for further discussion

the best fit line determined by this method is equal to $\left(2\sqrt{Dt}\right)^{-1}$ from which D can be calculated knowing t, the experimental duration.

Results

Zr diffusion in melt

The Zr diffusion measurements in LCO, LCl and MRF melts are listed in Table 2 and displayed in Figs. 2, 3 and 4. Measurements for melts with H_2O concentrations between approximately 4 and 5 wt% (Fig. 2) and melts containing between approximately 1.0 and 2.0 wt% H_2O (Fig. 3) were combined for each composition to calculate Arrhenius equations for high and low H_2O concentrations, respectively. Experiments performed for differing lengths of time on LCO at 1,200 °C (Table 2) yield diffusion coefficients and zircon solubilities that are either within error of each other, or are consistent with the effects of differing concentrations of FeO* and H_2O dissolved in the melt (discussed below). Although all melts lost water, this loss occurred early in the experiment (Freda et al. 2001)

Table 2 Experimental conditions and results. Numbers in parentheses are the standard deviations (1σ) based upon multiple analyses. Counting statistics for Zr at a concentration of ~2,000 ppm produce an uncertainty of ~170 ppm. FeO* concentrations have not been corrected for low totals because of the presence of water in the glasses. Experiments starting from AA29 were performed in a pyrophyllite-bearing assembly (see text). Zircon crystals used in experiments up to AA37 were from the Mud Tank Carbonatite (Australia); later experiments used zircon crystals from Colonia (Sri Lanka)

Sample	Temp. (°C)	Time (s)	FeO* (wt%)	H_2O[a] (wt%)	n[b]	C_o (ppm Zr)	D (m^2 s^{-1})
LCO							
AA6	1,050	154,800	0.72 (0.03)	3.92	3	875 (20)	$5.81\ (1.05)\times10^{-14}$
AA32	1,050	154,800	0.71 (0.03)	4.28	3	767 (52)	$5.13\ (2.64)\times10^{-14}$
AA3	1,200	72,000	0.64 (0.07)	3.05	3	2,100 (71)	$2.14\ (0.38)\times10^{-13}$
AA29	1,200	72,000	0.20 (0.02)	4.83	2	3,088 (619)	$6.06\ (6.28)\times10^{-13}$
AA37	1,200	28,800	0.67 (0.03)	4.52	3	2,738 (18)	$1.19\ (0.59)\times10^{-12}$
AA39[3]	1,200	28,800	0.20 (0.02)	4.48	3	2,325 (354)	$8.96\ (4.47)\times10^{-13}$
AA38	1,200	28,800	0.73 (0.03)	4.68	3	3,125 (35)	$1.69\ (0.58)\times10^{-12}$
AA9	1,400	7,200	0.08 (0.01)	3.54	3	11,492 (418)	$1.18\ (0.47)\times10^{-12}$
AA50	1,400	7,200	0.20 (0.01)	3.91	3	11,538 (336)	$1.02\ (0.06)\times10^{-12}$
AAX3	1,200	21,600	0.70 (0.04)	0.41	1	925	6.39×10^{-15}
AA12	1,200	72,000	0.66 (0.02)	0.56	2	1,500 (50)	$3.60\ (0.91)\times10^{-15}$
AA40[3]	1,200	28,800	0.60 (0.04)	1.78	3	2,742 (144)	$5.84\ (1.41)\times10^{-14}$
AA41	1,200	21,600	0.75 (0.03)	1.93	3	2,550 (863)	$4.98\ (1.49)\times10^{-14}$
AA16	1,300	18,000	0.44 (0.05)	0.63	3	5,100 (163)	$6.77\ (1.77)\times10^{-14}$
AA20	1,400	12,240	0.29 (0.13)	1.43	5	8,330 (361)	$2.35\ (0.44)\times10^{-13}$
AA53	1,400	12,240	0.54 (0.03)	1.59	3	5,200 (1,713)	$1.33\ (0.36)\times10^{-13}$
LCl							
AA4	1,050	154,800	0.64 (0.05)	3.69	3	905 (19)	$4.46\ (1.86)\times10^{-14}$
AA58	1,050	154,800	0.70 (0.04)	4.52	3	1,088 (194)	$4.60\ (1.74)\times10^{-14}$
AA1	1,200	72,000	0.76 (0.03)	3.54	3	3,067 (209)	$1.14\ (0.14)\times10^{-13}$
AA31	1,200	72,000	0.69 (0.02)	4.97	2	3,113 (407)	$1.48\ (0.16)\times10^{-13}$
AA24	1,400	7,200	0.02 (0.01)	3.05	2	10,613 (213)	$7.00\ (1.63)\times10^{-13}$
AA51	1,400	7,200	0.16 (0.02)	3.93	3	9,750 (468)	$3.12\ (0.60)\times10^{-12}$
AA10	1,200	72,000	0.76 (0.02)	0.51	2	1,538 (176)	$1.06\ (0.30)\times10^{-14}$
AAX1	1,200	21,600	0.65 (0.02)	0.91	3	1,617 (278)	$9.97\ (0.76)\times10^{-15}$
AA42	1,200	21,600	0.53 (0.05)	2.20	1	1,975	4.80×10^{-14}
AA28	1,400	3,780	0.74 (0.03)	0.66	4	7,500 (966)	$1.19\ (0.33)\times10^{-13}$
AA18	1,400	12,240	0.63 (0.02)	1.20	3	6,533 (392)	$1.09\ (0.15)\times10^{-13}$
AA54	1,400	12,600	0.70 (0.10)	0.99	3	6,850 (141)	$8.67\ (0.91)\times10^{-14}$
MRF							
AA5	1,050	154,800	1.69 (0.02)	4.90	4	916 (7)	$2.85\ (0.53)\times10^{-14}$
AA33	1,050	154,800	1.76 (0.05)	5.08	2	913 (159)	$5.23\ (1.03)\times10^{-14}$
AA2	1,200	72,000	1.85 (0.04)	3.34	3	1,983 (24)	$2.44\ (0.16)\times10^{-13}$
AA59	1,200	28,800	1.69 (0.04)	4.98	2	3,200 (212)	$2.14\ (1.24)\times10^{-13}$
AA27	1,400	3,780	1.65 (0.03)	4.46	3	11,267 (47)	$2.63\ (0.05)\times10^{-12}$
AA52	1,400	7,200	0.35 (0.02)	3.48	1	9,300	8.51×10^{-13}
AAX2	1,200	21,600	1.80 (0.03)	1.34	3	928 (33)	$6.94\ (0.08)\times10^{-14}$
AA11	1,200	72,000	1.78 (0.04)	1.99	3	2,333 (24)	$8.38\ (0.69)\times10^{-14}$
AA60	1,200	28,800	1.69 (0.14)	2.57	3	2,000 (566)	$4.50\ (1.47)\times10^{-14}$
AA15	1,300	18,000	1.59 (0.04)	1.17	3	3,350 (74)	$5.16\ (0.39)\times10^{-14}$
AA19	1,400	12,240	1.63 (0.07)	2.01	2	10,400 (495)	$3.85\ (0.14)\times10^{-13}$
AA55	1,400	12,600	0.74 (0.03)	2.42	3	7,700 (495)	$3.34\ (1.99)\times10^{-13}$

[a] H_2O measured by ion microprobe
[b] Number of traverses
[c] Experiments performed with graphite and pyrophyllite powder around the capsules (see text)

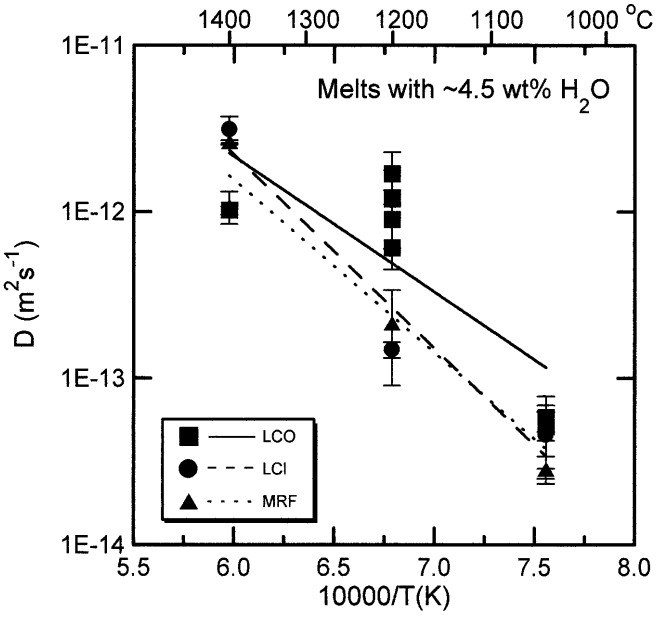

Fig. 2 Arrhenius diagram for diffusion of Zr in melts with ~4.5 wt% H_2O

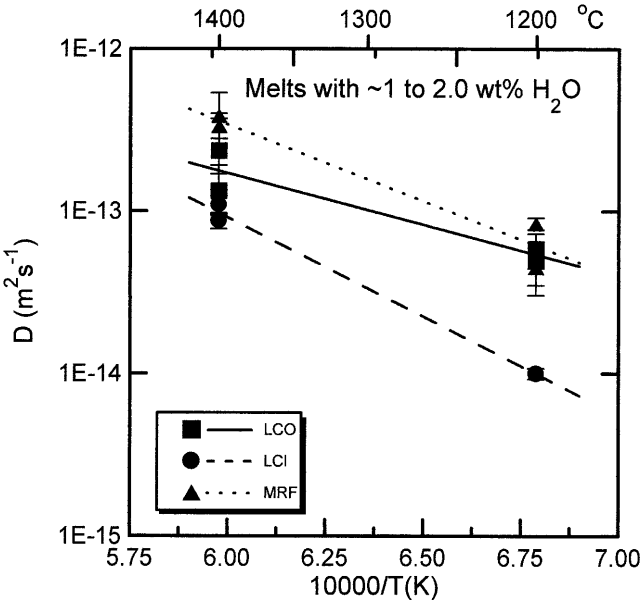

Fig. 3 Arrhenius diagram for diffusion of Zr in melts with ~ 2.0 wt% H_2O

and most of the diffusion occurred at the water concentrations measured by the ion microprobe. At a given temperature, H_2O concentration is the most important variable affecting Zr diffusion in the melts studied. Zirconium diffusion coefficients in the hydrous melts studied are at most only slightly affected by the presence of halogens at the concentration levels studied. The significant effect of H_2O, and the small effects of F and Cl, on Zr diffusion are best seen in Fig. 4a, b. At equivalent H_2O concentrations only small differences in Zr diffusion, typically less than a factor of 2, exist between the hydrous metaluminous melt, LCO and either the fluorinated, MRF, or chlorinated, LCl, melts.

In the temperature range investigated Zr diffusion in each melt behaves in an Arrhenian manner and can be described by:

$$D = D_o exp\left(\frac{-E_a}{RT}\right)$$

where D and D_o are in $m^2\ s^{-1}$, the activation energy is in kJ mol^{-1}, R is in J $mol^{-1}\ K^{-1}$, and T is in kelvin. Arrhenius equations were calculated using the technique of York (1969) and associated errors include uncertainties in temperature and diffusivity of individual experiments. Melts of the same anhydrous composition with similar measured water contents were grouped together such that the standard deviation about the mean water concentration was 0.5% absolute, or less. Although Zr diffusion coefficients in each base melt are similar, Zr diffusion in each melt with ~ 4.5 wt% H_2O can be described by its own Arrhenius line: for LCO with 4.4 ± 0.4 wt% H_2O (experiments AA-6, 32, 29, 37, 39, 38, 50):

$$D = 2.88 \pm 0.03x10^{-8} \exp\left(\frac{-140.1 \pm 33.9}{RT}\right)$$

for LCl with 4.5 ± 0.5 wt% H_2O (experiments AA-58, 31, 51):

$$D = 2.33 \pm 0.05x10^{-4} \exp\left(\frac{-254.8 \pm 64.1}{RT}\right)$$

and for MRF with 4.9 ± 0.3 wt% H_2O (experiments AA-5, 33, 59, 27):

$$D = 2.54 \pm 0.03x10^{-5} \exp\left(\frac{-223.8 \pm 15.5}{RT}\right)$$

When ~2 wt% H_2O is present in the melt, diffusion at any temperature is approximately 1.5–2 orders of magnitude below the diffusion measured in melts with 4.5 wt% H_2O (Table 2, Figs. 3 and 4), and the effect of added halogens remains minor. The Arrhenius equations describing diffusion in the melts with low H_2O concentrations are, for LCO with 1.7 ± 0.2 wt% H_2O (experiments AA-40, 41, 20, 53):

$$D = 5.39 \pm 0.2x10^{-9} \exp\left(\frac{-142.3 \pm 41.8}{RT}\right)$$

for LCl with 1.0 ± 0.2 wt% H_2O (experiments AAX1, AA-18, 54):

$$D = 1.87 \pm 0.04x10^{-6} \exp\left(\frac{-233.4 \pm 20.2}{RT}\right)$$

and, for MRF with 2.3 ± 0.3 wt% H_2O (experiments AA-11, 60, 19, 55):

$$D = 6.76 \pm 0.1x10^{-8} \exp\left(\frac{-168.0 \pm 22.4}{RT}\right)$$

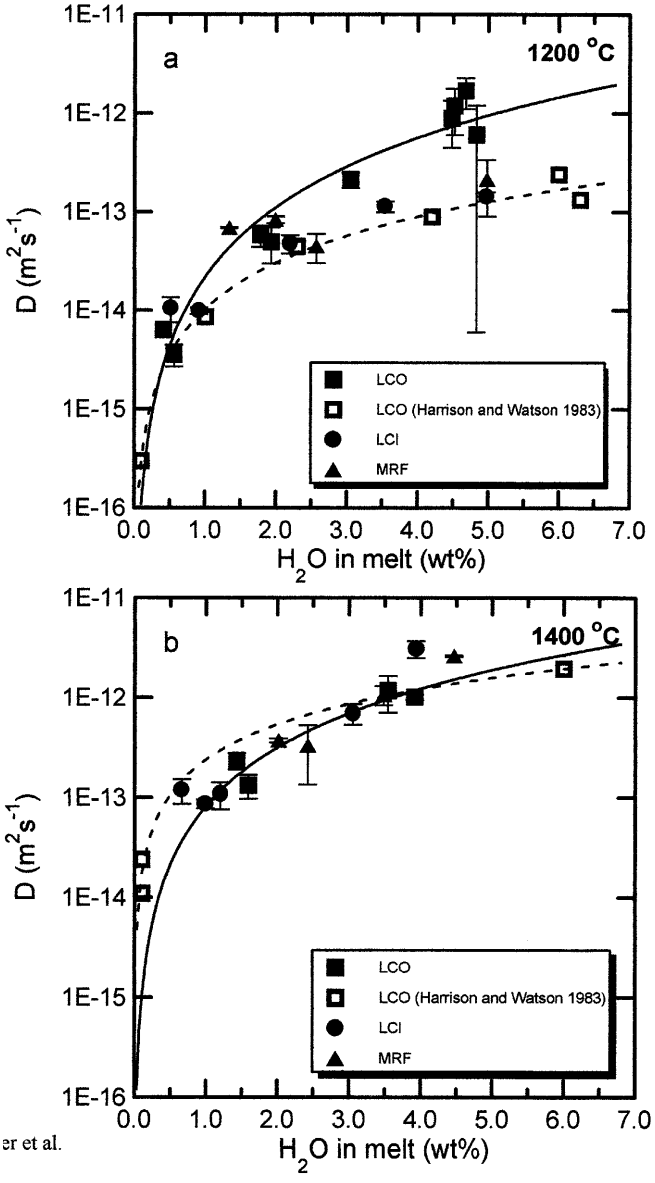

er et al.

Fig. 4 **a, b** Effect of H_2O concentration on Zr diffusion at **a** 1,200 °C and **b** 1,400 °C. *Solid line* is fit to Zr diffusion coefficients in LCO composition melt from this study and *dashed line* is fit to data from Harrison and Watson (1983) using the same composition

Zr concentration at zircon saturation

The concentration of Zr in LCO melt with ~4.5 wt% H_2O at zircon saturation, as determined by dissolution experiments, was reversed by crystallization experiments using LCOZr at 1,200 and 1,050 °C, 1.0 GPa (Table 3). Although the melt pools in these samples were too small for ion microprobe analysis, our study on water-loss from Au–Pd capsules at these conditions (Freda et al. 2001) constrains the H_2O contents of the melts to be 4.5 ± 0.5 wt%. At both temperatures the Zr concentrations in the zircon-saturated melt are within experimental uncertainty of the values measured using the dissolution technique.

Zircon solubility in melts with 4.5 wt% H_2O is little affected by the presence or absence of 1.2 wt% F or 0.35 wt% Cl at the conditions studied (Table 2). Solubilities range from 767 ppm at 1,050 °C to 11,538 ppm at 1,400 °C. These solubilities have been used to calculate the partition coefficient of Zr between zircon and melt, and plotted against 1/T (Fig. 5). At H_2O concentrations above 3 wt% the effect of adding additional water does not affect the Zr content of the melt by more than 10% relative (Fig. 6). Therefore, we have combined data from experiments with H_2O contents greater than 3 wt% for the calculation of Zr partition coefficient between zircon and melt, $D_{Zr}^{zircon/melt}$. The Zr partition coefficient in LCO can be described by:

$$\ln D_{Zr}^{zircon/melt} = 1.63\left(\frac{10000}{T}\right) - 5.87$$

for LCl by:

$$\ln D_{Zr}^{zircon/melt} = 1.47\left(\frac{10000}{T}\right) - 4.75$$

and for MRF by:

$$\ln D_{Zr}^{zircon/melt} = 1.47\left(\frac{10000}{T}\right) - 4.91$$

If all of the data with H_2O contents >3 wt% are averaged together, the resulting equation describing the partition coefficient is:

$$\ln D_{Zr}^{zircon/melt} = 1.53\left(\frac{10000}{T}\right) - 5.23$$

The solubility of zircon in melts containing ~2 wt% H_2O is lowered relative to melts with ~4.5 wt% H_2O (Table 2) and the partition coefficients correspondingly increased. The effect of increasing H_2O concentrations from ~0.5 to ~4.5 wt% decreases the Zr partition coefficient between zircon and melt by approximately a factor of 5 (Fig. 6). The MRF composition displays the smallest sensitivity of the partition coefficient to H_2O content.

Inspection of the concentrations of other elements along Zr diffusion profiles demonstrated homogenous melt compositions. In no case was evidence found to support either counter diffusion or complexing of Zr with halogens. Replicate experiments (AA37 and AA38) using the two different zircons produced consistent results.

Effects of FeO* and oxygen fugacity on zircon solubility

Two zircon dissolution samples using LCO melt, AA39 and AA40, were surrounded by a mixture of graphite + pyrophyllite powder during reaction at 1.0 GPa, 1,200 °C. The powder mixture was used to change the oxygen fugacity of the assembly from a value of approximately nickel–nickel oxide + 2 log units (Dalpé and Baker 2000) to a lower value, probably close to that of the wüstite–magnetite buffer (Dalpé and Baker 2000).

Table 3 Crystallization experiment conditions and results

Sample	Composition	T (°C)	Time (s)	FeO* (wt%)	Zr (ppm)	Comments
LHZr7	LCOZr	1,050	154,800	0.70 (0.02)[a]	938 (71)	1.0 GPa, ~4.5 wt% H_2O
LHZr5	LCOZr	1,200	72,000	0.69 (0.02)	2,722 (42)	1.0 GPa, ~4.5 wt% H_2O
LHZr6	LCOZrFe	1,200	72,000	4.18 (0.05)	2,909 (92)	1.0 GPa, ~4.5 wt% H_2O
AA68	LCOZrFe	1,400	72,000	4.53 (0.22)	12,257 (754)	0.1 MPa, $\log f_{O2} = -0.6$
AA66	LCOZrFe	1,400	72,000	4.31 (0.28)	13,431 (813)	0.1 MPa, $\log f_{O2} = -6.6$

[a]Uncertainties reported in parentheses are the standard deviations (1σ) about the means based upon a minimum of five analyses

Evidence of this lower oxygen fugacity is the observation that these samples suffered measurable iron loss at 1,200 °C. After the experiment, samples AA39 and AA40 contained 0.20 ± 0.02 and 0.60 ± 0.04 wt% FeO*, respectively. The loss of iron in AA39 resulted in a slightly decreased concentration of Zr at zircon solubility and diffusivity (Table 2). The small amount of iron lost from AA40 had no discernible effect on either Zr concentration or diffusion (Table 2). One experiment at the high oxygen fugacity that suffered iron loss (AA29, FeO* = 0.20 ± 0.02) does not appear to have a lower zircon solubility than similar experiments with higher FeO* concentrations at the same oxygen fugacity. However, this experiment has a high standard deviation on the Zr concentration at zircon solubility ($3{,}088 \pm 619$ ppm), which almost encompasses the zircon solubility value for AA39 ($2{,}325 \pm 354$ ppm Zr). The iron- and zirconium-enriched modification of LCO, LCOZrFe, was synthesized because of the equivocal evidence for the effect of oxygen fugacity and iron concentration on zircon saturation. An additional crystallization experiment at 1,200 °C, 1.0 GPa using LCOZrFe, demonstrated that changing FeO* from 0.69 to 4.18 wt% causes the Zr concentration to increase by approximately 200 ppm when compared with the LCO composition (Table 3). This increase is consistent with studies of zircon solubility in metaluminous haplogranitic systems at 1 atm, anhydrous conditions (Ellison and Hess 1986).

The effects of oxygen fugacity on zircon solubility were further explored by two preliminary experiments using the LCOZrFe composition at 1 atm and the lowest temperature at which successful experiments could be performed on this anhydrous composition, 1,400 °C (Table 3). (Experiments performed with LCOZr at this temperature produced heterogeneous glasses and were unsuitable, as were experiments with LCOZr and LCOZrFe at lower temperatures.) These experiments demonstrate that increasing oxygen fugacity 6 orders of magnitude from the wüstite–magnetite buffer to air decreases zircon solubility by 9% relative. These experiments demonstrate that oxygen fugacity can affect the solubility of zircon in silicic melts similar to LCO. However, to accurately quantify the effects of oxygen fugacity on zircon solubility requires a future set of solubility experiments at hydrous conditions in which both iron concentration and oxygen fugacity are well controlled.

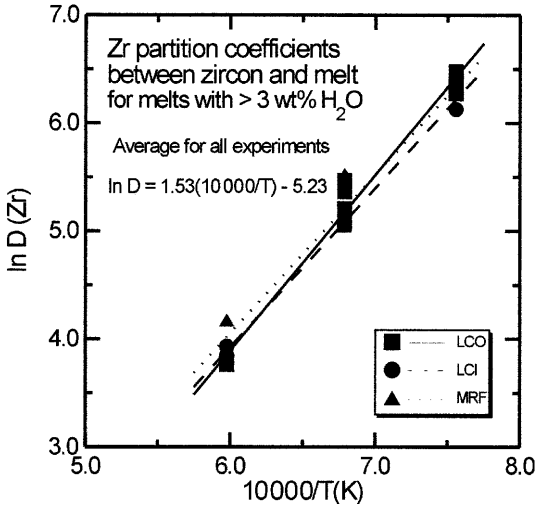

Fig. 5 Partition coefficients of Zr between zircon and melt for melts with greater than 3.0 wt% H_2O

Zr diffusion and concentrations in LCO melt at high temperatures and pressures: comparison with previous results

The Zr diffusivities measured in the halogen-free LCO melt with ~4.5 wt% H_2O (Fig. 4) are similar to previous measurements on the same composition with 6 wt% H_2O added (Harrison and Watson 1983) at 1,400 and 1,050 °C. Our 1,200 °C measurements are approximately a factor of 10 higher than those of Harrison and Watson (1983). The zirconium concentrations at zircon solubility are within error of those of Harrison and Watson (1983) at 1,400 °C, but at lower temperatures our values are consistently lower by approximately 30% relative at 1,200 °C (Fig. 6) and by a factor of 1.8 at 1,050 °C. These disagreements are not attributable to the difference in pressure between the experimental studies because pressure has been demonstrated to have an insignificant effect on zircon saturation (Watson and Harrison 1983). Nor can the differences be attributed to analytical problems because both Harrison and Watson (1983) and ourselves checked our analytical procedure by analysis of glasses with known zirconium concentrations.

The differences between our solubility results and those of Harrison and Watson (1983) are probably caused by different assemblies used in the piston-cylin-

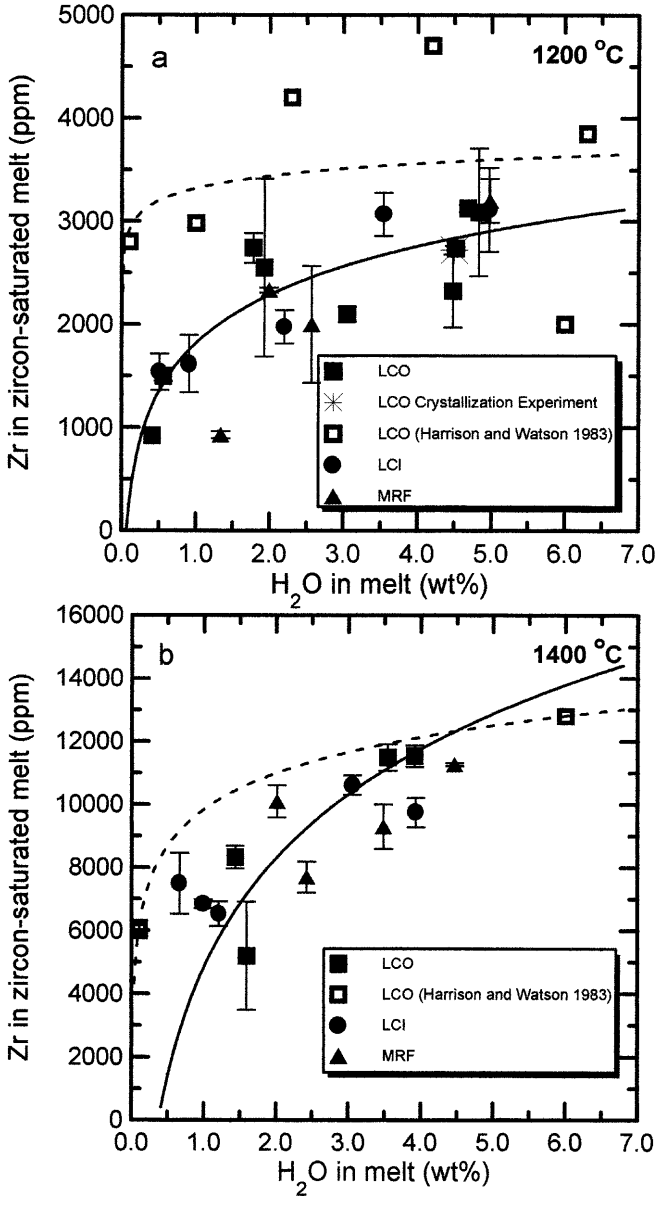

Fig. 6 a, b Effect of H_2O concentration on Zr values at zircon saturation at **a** 1,200 °C and **b** 1,400 °C. *Solid line* is fit to Zr solubility measurements in LCO composition melt from this study and *dashed line* is fit to data from Harrison and Watson (1983) using the same composition. Note, in Harrison and Watson's (1983) final analysis, the solubility data from the experiment at 1,200 °C with 6 wt% H_2O and 2,000 ppm Zr (ZIRDIS 7) was not used

der experiments. The assemblies of Harrison and Watson (1983) contained either internal pieces of unfired pyrophyllite (at 1,020 °C) or a pre-drilled graphite cylinder + pyrophyllite powder (at 1,200–1,400 °C, E.B. Watson 1999, personal communication). These assemblies differed substantially from those of this study and almost certainly resulted in a different oxygen fugacity than used in this study. The effect of oxygen fugacity on zircon solubility is hypothesized to be caused by its control of the Fe^{3+}/Fe^{2+} ratio in the melt. Ferric iron in silicate melts appears to behave as a network-former, whereas ferrous iron behaves as a network-modifier (Hess 1995). Thus as oxygen fugacity increases causing a concomitant increase in the Fe^{3+}/Fe^{2+} ratio, the proportion of network-formers in the melt should increase and the solubility of zircon decrease (cf. Ellison and Hess 1986). Our results on zircon solubility in LCOZrFe at 1 atm suggest that the oxygen fugacities in the experiments of Harrison and Watson (1983) were below ours and resulted in higher zircon solubilities than those measured in this study. The similarity of our results and those of Harrison and Watson (1983) at 1,400 °C indicate that either the effect of oxygen fugacity on zircon solubility decreases with temperature or that our different assemblies had similar oxygen fugacities at this temperature.

Geological implications

Zircon solubility at magmatic temperatures

The zirconium concentrations at zircon saturation in natural metaluminous, felsic melts are low, as previously demonstrated by Harrison and Watson (1983), Watson and Harrison (1983) and Keppler (1993). Because of the small effects of halogen addition (at the concentrations investigated) on zirconium content at zircon saturation, the partitioning data for all melts with >3 wt% H_2O was combined and extrapolated down to magmatic temperatures. The extrapolation predicts a solubility of 60 ppm at 800 °C and 14 ppm at 700 °C. The 800 °C value is within error of the Zr concentration determined by Keppler (1993), 67 ± 22 ppm, in a H_2O- (~6 wt%) and zircon-saturated haplogranitic melt at 800 °C and 200 MPa. However, this value is approximately one-third that for LCO melt calculated using the solubility data in Watson and Harrison (1983), 210 ppm (Fig. 7a). Even this value of 210 ppm is ~60 ppm lower than the expected value at zircon saturation based upon direct solubility measurements at 800 °C of Watson and Harrison (1983) (Fig. 7a). Even more problematical is the observation that solubilities calculated at 800 and 700 °C in this study are below the Zr concentrations of granitic and rhyolitic rocks known to contain no inherited zircons, only trace amounts of zircon phenocrysts. Examples of this discrepancy are the zircon-saturated, high-silica rhyolites of the classic Bishop Tuff (Hildreth 1981) whose low temperature member, ~720 °C, has a Zr concentration of 85 ppm, and whose high temperature member, ~790 °C, contains 145 ppm Zr (see Fig. 7).

We attribute differences between experiments and nature to the effects of iron concentration and oxygen fugacity. These effects on zircon saturation in metaluminous silicic melts have not been previously discussed, although Watson (1979) did note that addition of iron to peralkaline melts decreased the Zr concentration at zircon saturation.

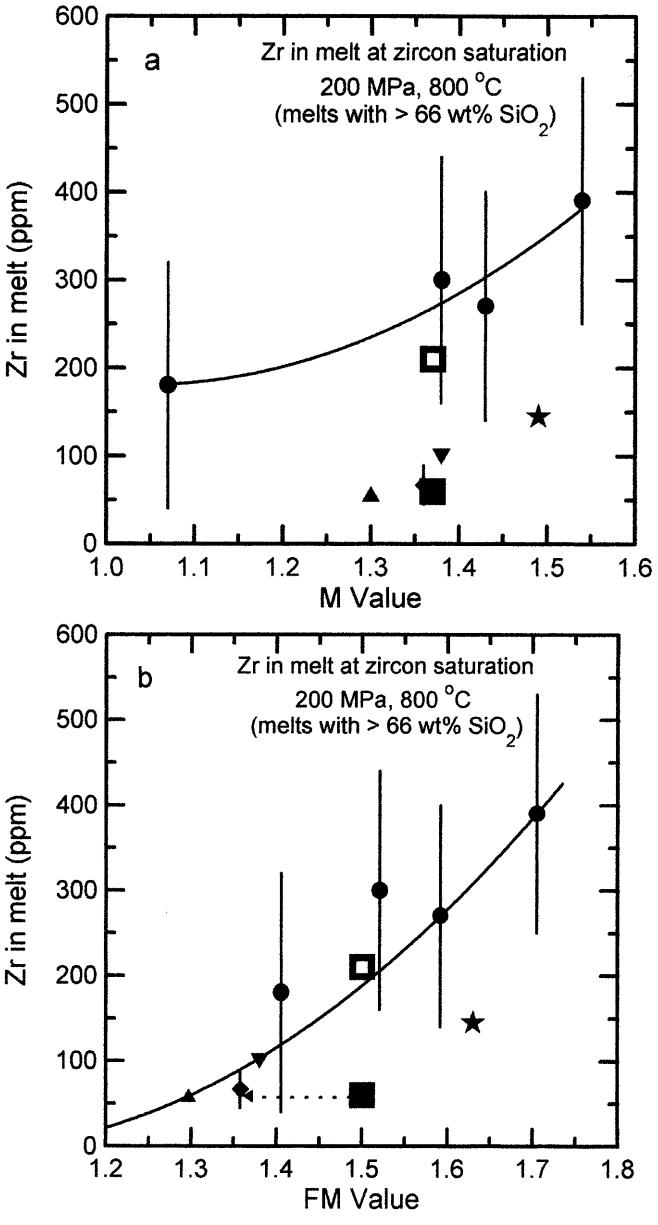

◀

Fig. 7 **a, b** Zr concentrations in melts saturated with zircon at 800 °C plotted as a function of **a** the M value and as a function of **b** the FM value. *Filled circles* are measurements from Watson and Harrison (1983), *diamond* is from Keppler (1993) at 800 °C, *upward pointing triangle* is from Larsen (1973) at 800 °C, the *downward pointing triangle* is the maximum value determined by Watson (1979) at 800 °C, the *star* is the high-temperature end member of the Bishop Tuff with an iron-oxide temperature of 790 °C (Hildreth 1981), the *filled square* is extrapolated from high-temperature measurements of saturation in LCO from this study and the *open square* is extrapolated from similar measurements in the same composition by Harrison and Watson (1983). See text for further discussion. In **a**, the *curve* is only a fit to the data of Watson and Harrison (1983) whereas in **b** the *curve* is fit to experimental solubility measurements at 800 °C, but not to extrapolations of LCO measurements. The *dashed line with the arrow* in **b** shows the effect on the FM value of treating all Fe in LCO as a network former and adding it to the value for Al in the denominator of the FM equation

The standard parameter used for describing the effects of melt composition on zircon saturation is the M parameter (Watson and Harrison 1983) based upon the cation ratio:

$$M = \frac{Na + K + 2Ca}{Al \cdot Si}$$

Although this parameter works well in many cases, it fails to provide a consistent means of predicting zircon saturation in iron-free melts at 800 °C (Fig. 7a). The solubility of these iron-free melts falls significantly below the correlation line between zircon saturation values of Zr in the melt and M (Fig. 7a). However, if the concentrations of Zr in melts saturated with zircon at 800 °C are plotted as a function of the FM cation ratio (Ryerson and Watson 1987), designed for the expression of rutile solubility:

$$FM = \frac{1}{Si} \cdot \frac{Na + K + 2(Ca + Mg + Fe)}{Al}$$

which includes the effects of Mg and total iron, but not the Fe^{3+}/Fe^{2+}, a smooth correlation between zircon saturation and the FM value can be constructed using measurements on iron-bearing melts (Harrison and Watson 1983) and iron-free melts (Larsen 1973; Watson 1979; Keppler 1993; Fig. 7b). When zircon saturation results for LCO are extrapolated to 800 °C and plotted as a function of FM (Fig. 7b), the value predicted by the data of Harrison and Watson (1983) falls almost upon the correlation line. However, the lower solubility data of this study are approximately one-third of that predicted by direct measurements at 800 °C; it should be noted that this value is within the uncertainty of the correlation curve between Zr in the melt at zircon saturation and the FM value. Although the use of the FM parameter is superior to that of the M parameter to describe the compositional variations that control zircon saturation, it fails to adequately treat the effects of the Fe^{3+}/Fe^{2+} ratio on zircon solubility and considers all iron in the melt to behave as a network modifier. If we consider all iron in LCO to be Fe^{3+} and treat it as a network former by adding it to aluminium in the denominator of the FM equation, then the position of LCO shifts to an FM value of 1.35 and the estimated solubility is consistent with direct saturation measurements at 800 °C (Fig. 7b). Unfortunately, we have not been able to measure the Fe^{3+}/Fe^{2+} ratio in our samples. Nevertheless, these results strongly suggest the need for a new parameter that describes the effects of major elements, H_2O, Fe^{2+}, Fe^{3+} and halogens on zircon saturation, but this must await future study.

Our data predict low values of Zr concentration at zircon saturation for magmatic temperatures because of differences in oxygen fugacity between our experiments and nature. Despite this observation, the relative values of the partition coefficients between zircon and melt between LCO, LCl and MRF should be reliable predictors of the effects of halogens on zircon saturation at

magmatic temperatures. The calculated Zr content in zircon-saturated melts at 800 °C with 4.5 wt% H_2O in LCO melt is 45 ppm, in MRF melt is 76 ppm and in LCl melt is 65 ppm. The small increase in zircon solubility with ~1 wt% fluorine addition to hydrous melts is consistent with the results of Keppler (1993); however, in both studies the increase in Zr concentration is within experimental uncertainty. We conclude that addition of halogens at concentrations typical of many metaluminous silicic rocks does not significantly affect the saturation of zircon in melts similar to those studied because of the insensitivity of the Zr partition coefficient to the addition of either 0.35 wt% Cl or 1.2 wt% F in melts containing 4.5 wt% H_2O. On the other hand, Keppler (1993) has conclusively demonstrated that higher concentrations of fluorine, 2–6 wt%, which are rare in nature (Carroll and Webster 1994), can substantially enhance the solubility of zircon.

Effects of halogens on Zr diffusion

The effect of addition of 0.35 wt% Cl or 1.2 wt% F to Zr diffusion in metaluminous granitic melts is minor (Figs. 2, 3 and 4). At 1,200 °C the addition of Cl or F decreases Zr diffusion by a factor of 0.5 at most. The increase in activation energy for Zr diffusion with the addition of either F or Cl to melts with ~4.5 wt% water is surprising because previous studies of hydrated, halogenated silicate melts demonstrated that F addition decreased activation energies for diffusion of major, non-alkali, elements (Baker and Bossànyi 1994). At the lower H_2O concentrations studied, the activation energies for Zr diffusion in LCO and LCl are similar to those at ~4.5 wt% H_2O, although the pre-exponential factors are smaller. MRF with 2.3 wt% H_2O displays both a lower activation energy and lower pre-exponential factor than when it contains 4.9 wt% H_2O. All of these observations relating the Arrhenius parameters to halogen and H_2O concentrations are presumably related to interactions between the halogens and the alkalies found in the zircono-silicate complexes in the melt (Watson 1979; Ellison and Hess 1986; Marr et al. 1998), rather than direct complexing with Zr (Farges 1996). The exact details of these interactions remain to be studied.

Extrapolation of the Arrhenius lines in melts with 4.5 wt% H_2O to a magmatic temperature of 800 °C produce Zr diffusivities of 4×10^{-15} in LCO, 3×10^{-16} in MRF, and 9×10^{-17} m^2 s^{-1} in LCl. The factor of 44 difference in diffusion at this temperature results in a factor of ~7 difference in the diffusion distance for a specific duration, using the estimation that $x=(Dt)^{1/2}$, where x is the distance, D is the diffusion coefficient, and t is the time. Extrapolation of Arrhenius equations for melts with 2 wt% H_2O is less precise than for those with 4.5 wt% H_2O because of the smaller temperature range studied. For melts with H_2O concentrations near 2 wt% the calculated diffusion coefficients at 800 °C are 6×10^{-16} for LCO, 5×10^{-16} for MRF, and 8×10^{-18} m^2 s^{-1} for LCl. The difference of a factor of 100 between the diffusion of Zr in LCO and in LCl results in diffusion differences of approximately 10 for a given time duration.

The dissolution of 100 μm zircon crystals into zircon-undersaturated melts at temperatures of 700 to 900 °C requires millions to billions of years if the granitic melt contains less than 0.5 wt% H_2O (Harrison and Watson 1983). If the H_2O concentration is increased to ~4.5 wt% the dissolution time for zircon in LCO drops to ~60 years at 900 °C and less than 2×10^4 years at 700 °C (Fig. 8). Halogen addition affects the dissolution rate of zircon crystals because of the halogens' effects on both Zr diffusion and zircon solubility in the melt. At 900 °C the zircon dissolution time in MRF is 228 years and in LCl is 701 years. The maximum difference in dissolution times between hydrous melts with and without halogens is a factor of 100 between LCO, 2×10^4 years, and LCl, 2×10^6 years, at 700 °C (Fig. 8). These calculations suggest that at temperatures of 800 °C and higher, the dissolution of zircons in any of the melts investigated will be geologically instantaneous. On the contrary, at the lowest temperature, during crustal melting, the presence of halogens can significantly affect the dissolution of zircon and diffusion of Zr in the melt.

Conclusions

The results of this study, combined with previous ones, on zircon solubility and Zr diffusion demonstrate that the significant variables affecting stability in granitic magmas are temperature, water content, total iron, ferric/ferrous and alkali/alumina ratios (Watson 1979; Harrison and Watson 1983; Watson and Harrison 1983;

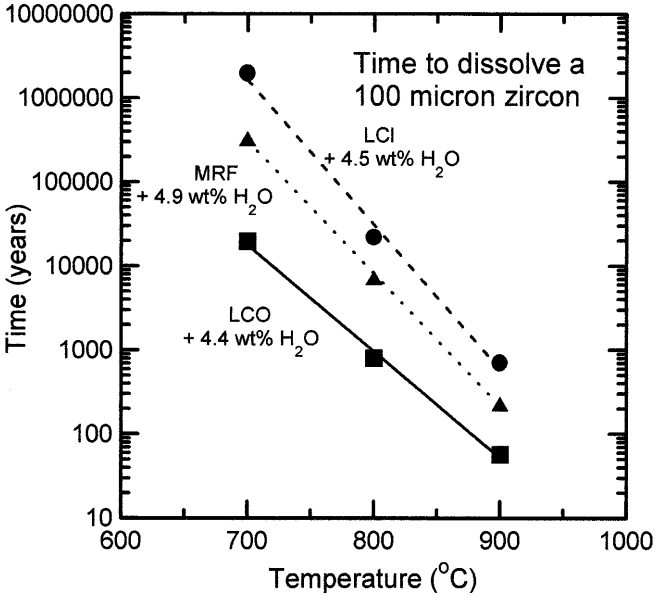

Fig. 8 Dissolution times for zircons in metaluminous granitic melts with differing halogen concentrations. Dissolution times were calculated assuming a 100-μm diameter spherical zircon crystal following equation 7.109 of Lasaga (1998)

Marr et al. 1998). Halogens dissolved in the melt at concentrations typically found in natural granitic or rhyolitic rocks, near to or less than 1 wt%, exert a small effect on the solubility of zircon and the diffusion of Zr in the melt. At the experimental conditions the effects of halogen addition are difficult to measure, but when the Arrhenius lines for melts with $\sim$ 4.5 wt% H_2O are extrapolated to magmatic temperatures, Zr diffusion in the chlorinated melt is reduced compared with the halogen free and zfluorine-bearing melts. At 700 °C, Zr diffusion in the Cl-bearing melt is 1/100th of that in the halogen-free melt. Nevertheless, the effect of halogens on zircon solubility and diffusion of Zr in granitic melts is minor, and probably geologically unimportant at temperatures greater than 800 °C. Thus, the presence of small amounts of halogens in felsic rocks probably cannot explain the possible correlation between Zr and halogens sometimes observed.

Acknowledgements We give a heartfelt thanks to T.M. Harrison for a thorough and educational review and to E.B. Watson for inspirational discussions over e-mail. We wish to thank G. Poirier for assistance on the electron microprobe, A. Gibbs for help with the experiments and M. Simpson for valuable advice. This research was funded by NSERC grants OGP89662 and CPG0183275, FCAR Soutien aux équipes de recherche, CNR grant Bando n.203.05.18 to C.F., and CNR Short-Term Mobility Program 1998 to A.M.C. Finally, the Consiglio Nazionale delle Ricerche is acknowledged for financing the ion microprobe at CSCC (Pavia) whose facility was used in the present work.

References

Baker DR, Bossànyi H (1994) The combined effect of F and H_2O on interdiffusion between peralkaline dacitic and rhyolitic melts. Contrib Mineral Petrol 117:203–214

Baker DR, Vaillancourt J (1995) The low viscosities of F + H_2O-bearing granitic melts and implications for melt extraction and transport. Earth Planet Sci Lett 132:199–211

Carroll MR, Webster JD (1994) Solubilities of sulfur, noble gases, nitrogen, chlorine, and fluorine in magmas. In: Carroll MR, Holloway JR (eds) Volatiles in magmas. Min Soc Am Rev Mineral 30:231–279

Congdon RD, Nash WP (1991) Eruptive pegmatite magma: rhyolite from the Honeycomb Hills, Utah. Am Mineral 76:1261–1278

Conrad WK (1984) The mineralogy and petrology of compositionally zoned ash flow tuffs, and related silicic volcanic rocks, from the McDermitt Caldera Complex, Nevada–Oregon. J Geophys Res 89:8639–8664

Crank J (1975) The mathematics of diffusion. Clarendon Press, Oxford

Dalpé C, Baker DR (2000) Experimental investigation of LILE, HFSE, and REE partitioning between calcic amphibole and basaltic melt: the effects of pressure and oxygen fugacity. Contrib Mineral Petrol 140:233–250

Eichorn R, Loth G, Höll R, Finger F, Shermaier A, Kennedy A (2000) Multistage Variscan magmatism in the Tauren Window (Austria) unveiled by U/Pb SHRIMP zircon data. Contrib Mineral Petrol 139:418–435

Ellison AJ, Hess PC (1986) Solution behavior of +4 cations in high silica melts: petrologic and geochemical implications. Contrib Mineral Petrol 94:343–351

Farges F (1996) Does Zr–F 'complexation' occur in magmas? Chem Geol 127:253–268

Fourcade S, Allegre CJ (1981) Trace elements behavior in granite genesis: a case study. The calc-alkaline plutonic association from the Querigut Complex (Pyrénées, France). Contrib Mineral Petrol 76:177–195

Freda C, Baker DR, Ottolini L. (2001) Reduction of water loss from gold-palladium capsules during piston-cylinder experiments by use of pyrophyllite powder. Am Mineral 86:234–237

Green TH, Watson EB (1982) Crystallization of apatite in natural magmas under high pressure hydrous conditions, with particular reference to orogenic rock series. Contrib Mineral Petrol 79:96–105

Hanson GN (1978) The application of trace elements to the petrogenesis of igneous rocks of granitic composition. Earth Planet Sci Lett 38:26–43

Harrison TM, Watson EB (1983) Kinetics of zircon dissolution and zirconium diffusion in granitic melts of variable water content. Contrib Mineral Petrol 84:66–72

Harrison TM, Watson EB (1984) The behavior of apatite during crustal anatexis: equilibrium and kinetic considerations. Geochim Cosmochim Acta 48:1467–1477

Hervig RL, Dunbar NW (1992) Cause of chemical zoning in the Bishop (California) and Bandelier (New Mexico) magma chambers. Earth Planet Sci Lett 111:97–108

Hess PC (1995) Thermodynamic mixing properties and the structure of silicate melts. In: Stebbins JF, McMillan PF, Dingwell DB (eds) Structure, dynamics and properties of silicate melts. Mineral Soc Am Rev Mineral 32:145–189

Hildreth W (1981) Gradients in silicic magma chambers: implications for lithospheric magmatism. J Geophys Res 86:10153–10192

Hildreth W, Christiansen RL, O'Neil JR (1984) Catastrophic isotopic modification of rhyolitic magma at times of caldera subsidence, Yellowstone Plateau field. J Geophys Res 89:8339–8369

Hildreth W, Halliday AN, Christiansen RL (1991) Isotopic and chemical evidence concerning the genesis and contamination of basaltic and rhyolitic magma beneath the Yellowstone Plateau volcanic field. J Petrol 32:63–138

Hoskin PWO, Kinny PD, Wyborn D, Chappell BW (2000) Identifying accessory mineral saturation during differentiation in granitoid magmas: an integrated approach. J Petrol 41:1365–1396

Hudon P, Baker DR, Toft PB (1994) A high-temperature assembly for 1.91-cm (3/4 in.) piston-cylinder apparatus. Am Mineral 79:145–147

Keppler H (1993) Influence of fluorine on the enrichment of high field strength trace elements in granitic rocks. Contrib Mineral Petrol 114:479–488

Keppler H, Wyllie PJ (1990) Role of fluids in transport and fractionation of uranium and thorium in magmatic processes. Nature 348:531–533

Keppler H, Wyllie PJ (1991) Partitioning of Cu, Sn, Mo, W, U and Th between melt and aqueous fluid in the system haplogranite–H_2O–HCl and haplogranite–H_2O–HF. Contrib Mineral Petrol 109:139–150

Larsen L (1973) Measurement of solubility of zircon ($ZrSiO_4$) in synthetic granitic melts. Trans Am Geophys Union 54:479

Lasaga AC (1998) Kinetic theory in the Earth sciences. Princeton University Press, Princeton

London D (1987) Internal differentiation of rare element pegmatites: effects of boron, phosphorous, and fluorine. Geochim Cosmochim Acta 51:403–420

Marr RA, Baker DR, Williams-Jones AE (1998) Chemical controls on the solubility of Zr-bearing phases in simplified peralkaline melts and application to the Strange Lake Intrusion, Quebec – Labrador. Can Mineral 36:1001–1008

Miller CF, Mittlefehldt DW (1982) Depletion of high rare-earth elements in felsic magmas. Geology 10:129–133

Mittlefehldt DW, Miller CF (1983) Geochemistry of the Sweetwater Wash Pluton, California: implications for 'anomalous' trace element behavior during differentiation of felsic magmas. Geochim Cosmochim Acta 47:09–124

Mutschler FE, Rougon DJ, Lavin OP, Hughes RD (1981) Petros–a data bank of major element chemical analyses of igneous

rocks for research and teaching (version 6.1). Boulder Colorado, NOAA – National Geophysical Data Center
Nasdala L, Götze J, Pidgeon RT, Kempe U, Seifert T (1998) Constraining a SHRIMP U–Pb age: micro-scale characterization of zircons from Saxonian Rotliegend rhyolites. Contrib Mineral Petrol 132:300–306
Newman S, Stolper EM, Epstein S (1986) Measurement of water in rhyolitic glasses: calibration of an infrared spectroscopic technique. Am Mineral 71:1527–1541
Ottolini L, Bottazzi P, Zanetti A, Vannucci R (1995) Determination of hydrogen in silicates by secondary ion mass spectrometry. Analyst 120:1309–1313
Pichavant M, Herrera JV, Boulmier S, Briqueu L, Joron JL, Juteau M, Marin L, Michard A, Sheppard SMF, Treuil M, Vernet M (1987) The Macusani glasses SE Peru: evidence of chemical fractionation in peraluminous magmas. In: Mysen BO (Ed) Magmatic processes: physiochemical principles. Special publication 1. Geochemical Society, University Park, Pennsylvania, pp 359–373
Pidgeon RT, Bosch D, Bruguier O (1996) Inherited zircon and titanite U–Pb systems in an Archaean syenite from Southwestern Australia: implications for U–Pb stability of titanite. Earth Planet Sci Lett 141:187–198
Pidgeon RT, Nemchin AA, Hitchen GJ (1998) Internal structures of zircons from Archean granites from the Darling Range batholith: implications for zircon stability and the interpretation of zircon U–Pb ages. Contrib Mineral Petrol 132:288–299
Pollard PJ, Pichavant M, Charoy B (1987) Contrasting evolution of fluorine- and boron-rich tin system. Miner Deposita 22:315–321
Raimbault L, Meyer G, Treuil M (1987) Comportements differenciés de W, Sn, U, Ta, Nd dans quelques complexes granitiques du Massif Central Français. Bull Minéral 110:591–601
Rapp RP, Watson EB (1986) Monazite solubility and dissolution kinetics: implication for the thorium and light rare earth chemistry of felsic magmas. Contrib Mineral Petrol 94: 304–316
Ryerson FJ, Watson EB (1987) Rutile saturation in magmas: implications for Ti–Nb–Ta depletion in island-arc basalts. Earth Planet Sci Lett 86:225–239
Rytuba JJ, McKee EH (1984) Peralkaline ash flow tuffs and calderas of the McDermitt Volcanic Field, south east Oregon and north central Nevada. J Geophys Res 89:8616–8628
Schaller T, Dingwell DB, Keppler H, Knöller W, Merwin L, Sebald A (1992) Fluorine in silicate glasses: a multinuclear nuclear magnetic resonance study. Geochim Cosmochim Acta 56:701–707
Štemprok M (1991) Ongonite from Ongon Khairkhan, Mongolia. Mineral Petrol 43:255–273
Watson EB (1979) Zircon saturation in felsic liquids: experimental results and application to trace element geochemistry. Contrib Mineral Petrol 70:407–419
Watson EB (1980) Some experimentally-determined zircon/liquid partition coefficient for the rare-earth elements. Geochim Cosmochim Acta 44:895–897
Watson EB, Capobianco CJ (1981) Phosphorous and the rare-earth elements in felsic magmas: an assessment of the role of apatite. Geochim Cosmochim Acta 45:2349–2358
Watson EB, Green TH (1981) Apatite/liquid partition coefficients for the rare earth elements and strontium. Earth Planet Sci Lett 56:405–421
Watson EB, Harrison TM (1983) Zircon saturation revisited: temperature and composition effects in a variety of crustal magma types. Earth Planet Sci Lett 64:295–304
Webster JD (1992) Water solubility and chlorine partitioning in Cl-rich granitic systems: effects of melt composition at 2 kbar and 800 °C. Geochim Cosmochim Acta 56:659–678
York D (1969) Least squares fitting on a straight line with correlated errors. Earth Planet Sci Lett 5:320–324